



Published in final edited form as:

Photochem Photobiol. 2016 July ; 92(4): 620–623. doi:10.1111/php.12592.

Promotion of Pro-Apoptotic Signals by Lysosomal Photodamage: Mechanistic Aspects and Influence of Autophagy

David Kessel^{1,*} and Conor L. Evans²

¹Department of Pharmacology, Wayne State University, Detroit, MI 48201

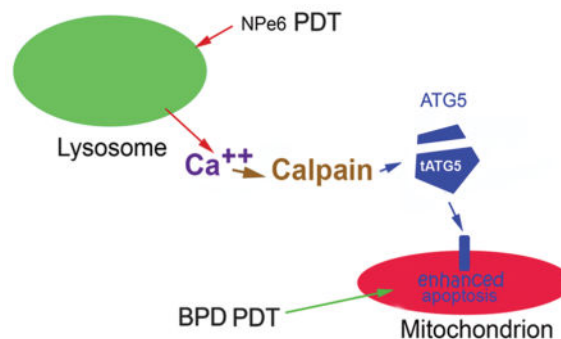
²Wellman Center for Photomedicine, Harvard Medical School Massachusetts General Hospital, Boston MA 02128

Abstract

Prior studies demonstrated that a low level (LD₁₀₋₁₅) of lysosomal photodamage can sensitize cells to the apoptotic death that results from subsequent mitochondrial photodamage. We have proposed that this process occurs via a calpain-catalyzed cleavage of the autophagy-associated protein ATG5 to form a pro-apoptotic fragment. In this report, we provide evidence for the postulated ATG5 cleavage and show that the sequential photodynamic therapy (PDT) protocol can also partly overcome the adverse effect of hypoxia on the initiation of apoptosis. While autophagy can offer cytoprotection after mitochondrial photodamage, this does not appear to apply when lysosomes are the target. This may account for the ability of very low PDT doses directed at lysosomes to evoke ATG5 cleavage. The resulting pro-apoptotic effect overcomes intrinsic cytoprotection from mitochondrial photodamage along with a further stimulation of phototoxicity.

Scheme whereby release of calcium from photodamaged lysosomes activates calpain. This enzyme then catalyzes activation of calpain. This enzyme then cleaves the autophagy associated protein ATG5 to a truncated form that potentiates the initiation of apoptotic death after a subsequent PDT dose directed at mitochondria. The net result is substantially enhanced photokilling that can circumvent sub-optimal delivery of light and oxygen.

Graphical abstract



*Corresponding author: dhkessel@med.wayne.edu (David Kessel).

INTRODUCTION

Use of photosensitizing agents and light to produce a cytotoxic effect is termed photodynamic therapy (PDT) (1,2). PDT is mediated by reactive oxygen species (ROS) formed during the irradiation process. These reactive oxygen species have a very short (microsecond) half-life with photodamage is limited to the subcellular sites where the photosensitizing agent initially localizes. Photosensitizers are available with a range of specific targets making it feasible to direct photodamage to specific sub-cellular organelles.

We previously reported that a low level of lysosomal photodamage could markedly potentiate the efficacy of subsequent mitochondrial photodamage *in vitro*. (3–5). A similar sequential PDT result was reported in 1996 involving a murine sarcoma model *in vivo*, but no persuasive mechanism was advanced (6). We proposed low-level lysosomal photodamage led to promotion of pro-apoptotic signals, an effect initially described in studies on the autophagy-related gene termed ATG5 by Simon's group (7). This mechanism involves a calpain-catalyzed cleavage of ATG5 to form a pro-apoptotic fragment. Since lysosomes are a reservoir for Ca^{2+} (8), lysosomal photodamage was proposed to be the initiating factor that triggers calpain activation. We also explored the possible involvement of autophagy: this process can provide a cytoprotective response to photodamage after mitochondrial photodamage, but not when lysosomes are the initial PDT target.

MATERIALS AND METHODS

Chemicals and supplies

NPe6 was provided by Dr. Kevin M. Smith, Louisiana State University. BPD (benzoporphyrin derivative, Verteporfin) was purchased from VWR (Cat No 1711461). Other reagents were obtained from Sigma-Aldrich and were of the highest available purity. Fluorescent probes were provided by Life Technologies, Inc.

Cell culture and clonogenic assays

Growth of murine hepatoma 1c1c7 cells and procedures for clonogenic assays have been described previously (9). Irradiation was carried out in air (20% oxygen) or in a system equilibrated with an atmosphere of 1% oxygen, 99% nitrogen provided by a hypoxia chamber (Biospherix Inc., Lacona, NY). As in previous studies, media buffered to pH 7.2 with HEPES was used for all *in vitro* operations so that the absence of CO_2 did not affect maintenance of pH.

PDT protocols

Cell cultures on cover slips in 30 mm diameter sterile plastic dishes were incubated at 37°C with 20 or 40 μM NPe6 for 1 h. Where indicated, 0.5 μM BPD was added concurrently with NPe6. The medium was replaced and the dishes irradiated using a 600-watt quartz-halogen source filtered through 10 cm of water to remove wavelengths of light > 900 nm. The bandwidth was further confined by interference filters (Oriel, Stratford CT) to 660 ± 10 nm (90 or 180 mJ/cm^2) for NPe6. Where specified, this was immediately followed by irradiation at 690 ± 10 nm (37.5 mJ/cm^2) to initiate BPD-induced mitochondrial photodamage. To

achieve these PDT doses, the irradiation times were 60 or 120 sec at 660 nm and 25 sec at 690 nm.

Microscopy protocols

Loss of the mitochondrial membrane potential (Ψ_m) was assessed by fluorescence microscopy using the probe mitotracker orange (MTO) as described in Ref 10. Images were acquired with a Nikon E-600 microscope using a Rolera EM-CCD camera and MetaMorph software (Molecular Devices, Sunnyvale CA). MTO fluorescence was detected using a Nikon 'B' filter combination (excitation 510–560 nm, emission at wavelengths >590 nm). A 650 nm low-pass filter was placed in the emission beam to prevent photosensitizer fluorescence from reaching the CCD camera. At least 3 images were acquired for each sample, with typical representations shown here.

Western blots

Cells were lysed in SDS-PAGE buffer containing a collection of protease inhibitors (Sigma-Aldrich S8830). The lysate was then heated to 100°C for 5 min. Aliquots containing 40 μ g of protein per well were used for western blot analysis. For the ATG5 studies, the truncated ATG5 fragment represents amino acids 1–193 from the 276 that comprise ATG5. The antibody used for detection (Abgent) was raised against residues 1–30 at the N-terminal end and 209–238 toward the C-terminal end. This can detect both ATG5 and the 24 kDa fragment (7). Simon (personal communication) reported that this fragment is unstable and requires the presence of protease inhibitors during isolation procedures. For assessing level of LC3 I and II, an antibody to the murine LC3 protein was provided by Proteintech Group, Inc., Chicago, IL. Electrophoresis was carried out on 4–10% tris-glycyl acrylamide gels and the proteins transferred to polyvinylidene fluoride membranes. The membranes were probed with the specified antibody, followed by a 1 hr incubation with an alkaline phosphatase-coupled secondary antibody at room temperature (Vistra ECF western blot reagent, Amersham). A substrate is then cleaved by phosphatase activity to form a fluorescent product that is detected with a Storm imaging system (Molecular Dynamics).

Autophagic flux

During autophagy, there is conversion of the protein termed LC3-I to a lipidated form termed LC3-II. If autophagy is impaired, LC3-II will accumulate. Degradation of LC3-II can also be blocked by the drug bafilomycin permitting an estimate of the autophagic flux (15). In these studies, the autophagic flux was monitored by observing the relative levels of LC3-II formed during a 1 hr interval in the absence vs. presence of 100 nM bafilomycin.

DEVDase assays

Cells were collected 2 h after irradiation and assayed for DEVDase activity (11). This DEVDase activity represents the activation of pro-caspases 3/7, a hallmark of apoptosis. A kit provided by Invitrogen was used for this purpose (cat. no. E13184). Enzyme levels are reported in terms of nmol product/min/mg protein. Each assay was performed in triplicate. The Micro Lowry assay was used to estimate protein concentrations, using bovine serum albumin as the standard.

RESULTS AND DISCUSSION

Effects of NPe6/BPD PDT on the Ψ_m and survival

In a previous report, the effect of the combination protocol on survival was estimated by measuring loss of the mitochondrial membrane potential (Ψ_m); the results were well-correlated with clonogenic assays for photokilling (10). In the original report (4), we showed that a 40 μM concentration of NPe6, followed by a 90 mJ/cm^2 light dose at 660 nm was capable of sensitizing 1c1c7 cells to mitochondrial photodamage induced by BPD. Decreasing the NPe6 concentration by 50% and doubling the light dose had a similar effect (Fig. 1). Either protocol: (20 μM NPe6 combined with 180 mJ/cm^2 of light or 40 μM / 90 mJ/cm^2) led to a substantial promotion of photokilling by BPD (Fig. 2). This does not appear to be associated with any changes in BPD accumulation or localization caused by lysosomal photodamage initiated by NPe6 (3). For the optimal potentiation of photokilling, lysosomal photodamage must precede PDT directed at mitochondria (3), a phenomenon also encountered by Cincotta *et al* (6). This implies that the pro-apoptotic effects of the ATG5 fragment are transitory.

Photodamage causes the formation of an ATG5 fragment

The pro-apoptotic nature of lysosomal photodamage is hypothesized to arise from calpain-dependent cleavage of protein ATG5, which then acts to potentiate cell death from further mitochondrial photodamage. Studies by Simon's group and others have investigated the pro-apoptotic consequences of formation of an ATG5 24 kDa fragment (7,12,13). To see if this fragment is formed after NPe6 lysosomal photodamage, cells were incubated with 40 μM NPe6 and irradiated using the 90 mJ/cm^2 . In the presence of protease inhibitors, we were able to detect this fragment directly after low-dose lysosomal photodamage (Fig. 3). While the level detected was not large, this is consistent with prior reports cited above: a relatively minor formation of the ATG5 fragment appears to have significant pro-apoptotic efficacy.

Ability of sequential protocol to compensate for effects of hypoxia on DEVDase activity

Photodamage directed at lysosomes or mitochondria can provoke activation of 'executioner' caspases (3 and 7) that ultimately lead to apoptotic death. Prior studies carried out in 20% oxygen indicated that the PDT dose of BPD used in these studies resulted in photokilling of ~15% of the population while the combination with NPe6 led to a 90% cell kill (3). Irradiation of cells in a hypoxic environment (1% oxygen) had a minimal effect on DEVDase activation using NPe6 alone, consistent with a previous report (14). We observed a greater sensitivity to hypoxia using BPD as the photosensitizing agent (Fig. 4). A prior low level of lysosomal photodamage markedly potentiated caspase activation by BPD under normoxic conditions. Even under 1% oxygen an effect was observed although the magnitude was clearly reduced. We conclude that the sequential protocol can promote PDT efficacy even when the oxygen concentration level is reduced to 1%.

Dark effects of NPe6 on the autophagic flux

To assess effects of NPe6 on autophagy in the dark, the autophagic flux was monitored by comparing LC3-II levels in the presence vs. absence of bafilomycin. In control cells, a

marked increase in the concentration of this protein was observed. This increase was unaffected by 20 μM NPe6 but inhibited by a 40 μM concentration in the dark (Fig. 5).

Lysosomal vs. mitochondrial photodamage: effects of autophagy

In prior reports (9,16), we compared the effect of autophagy on the dose response curves involving PDT and mitochondrial vs. lysosomal targets. The results indicate a cytoprotective effect of autophagy after mitochondrial photodamage, represented by a shoulder on the dose-response curve that was absent when autophagy was impaired. In contrast, no such effect was observed when lysosomes were the sole PDT target. In the latter study, the NPe6 concentration was 20 μM , a concentration shown (Fig. 5) not to impair the autophagic flux.

CONCLUSIONS

A 1996 report indicated that a photodynamic therapy protocol, involving two photosensitizing agents, resulted in a significantly higher degree of tumor eradication than could be achieved with either photosensitizer alone (6). An optimal response observed only when lysosomal photodamage preceded mitochondrial targeting. We have proposed that cleavage of ATG5 to a pro-apoptotic fragment after lysosomal photodamage explains the enhanced efficacy of this protocol. It appears that limitations to cancer control resulting from inadequate light doses or hypoxia can thereby be circumvented. The low level of lysosomal photodamage is insufficient to alter the pH gradient responsible for the localization of the fluorescent LysoTracker green (LTG) label (4), but appears sufficient to initiate ATG5 cleavage (Fig. 3).

We propose that data described in Refs. 9 and 16 have further significance. Autophagy is known to exert a cytoprotective effect after mitochondrial photodamage (9,17). Lemasters had proposed that an autophagic process can sequester mitochondria before cytochrome c can be released (18). Such a cytoprotective effect was not observed when lysosomes were the PDT target (16). This may account for the ability of low-dose lysosomal photodamage to have such a profound effect. Absence of autophagic cytoprotection may also be responsible for the greater efficacy when lysosomes, rather than mitochondria, are the PDT target (19).

Other studies indicate that autophagy is unable to offer significant protection from photokilling by the sequential protocol, i.e., the sequential protocol overcomes the cytoprotective effect of autophagy after mitochondrial photodamage. While some of our earlier studies utilized a high concentration of NPe6 (3,4), we show here that a lower NPe6 concentration, using a higher light dose, has a similar effect. We had previously used a specific PI3K antagonist to demonstrate that autophagy was likely not a factor in the efficacy of the sequential protocol (3). Use of such antagonists to rule out an autophagic effect has, however, been questioned (20). In this study, we provide additional evidence. Use of an NPe6 concentration that can antagonize autophagy, as described in Ref. 21 and illustrated in Fig. 5, was no more or less effective than a lower NPe6 concentration (Fig. 2) that does not affect the autophagic flux (Fig. 5). Based on the mechanism proposed by Simon's group (7), along with results reported here (Fig. 3) and elsewhere (3–5), we propose that the results obtained with the sequential PDT protocol can best be explained by a mechanism resulting

in cleavage of ATG5 to a pro-apoptotic fragment that enhances photokilling after mitochondrial photodamage.

The use of lysosomal PDT to potentiate apoptosis has the potential to play a role across a number of therapeutic regimens, and may be beneficial in combination with chemotherapy agents. Interestingly the potentiation of apoptosis by lysosomal photosensitization may be especially helpful in amplifying the effects of already-existing intracellular reactive oxygen species. As high intracellular reactive oxygen species have been implicated in limiting the spread of certain cancers (22,23), a low-level lysosomal PDT regimen could serve to further tip the scales toward apoptotic death. Furthermore, the cleavage of the ATG5 fragment after a low level of lysosomal damage suggests a potential drug target for future combination therapies.

Acknowledgments

This study was partly supported by grant CA23378 from the National Cancer Institute, National Institutes of Health. CLE was supported by the NIH Director's New Innovator Award, grant DP2 OD007096. Information on the New Innovator Award program is at <http://nihroadmap.nih.gov/newinnovator/>. We thank Ann Marie Santiago for excellent technical assistance.

References

1. Dougherty TJ, Gomer CJ, Henderson BW, Jori G, Kessel D, Korbek M, Moan J, Peng Q. Photodynamic therapy. *J Natl Cancer Inst.* 1998; 90:889–905. [PubMed: 9637138]
2. Agostinis P, Berg K, Cengel KA, Foster TH, Girotti AW, Gollnick SO, Hahn SM, Hamblin MR, Juzeniene A, Kessel D, Korbek M, Moan J, Mroz P, Nowis D, Piette J, Wilson BC, Golan J. Photodynamic therapy of cancer: an update. *CA Cancer J Clin.* 2011; 61:250–281. [PubMed: 21617154]
3. Kessel D, Reiners JJ Jr. Enhanced efficacy of photodynamic therapy via a sequential targeting protocol. *Photochem Photobiol.* 2014; 90:889–895. [PubMed: 24617972]
4. Kessel D, Reiners JJ Jr. Promotion of Proapoptotic Signals by Lysosomal Photodamage. *Photochem Photobiol.* 2015; 91:931–936. [PubMed: 25873082]
5. Kessel D. Photodynamic therapy: promotion of efficacy by a sequential protocol. *J Porph Phthalo.* 2016 In Press.
6. Cincotta L, Szeto D, Lampros E, Hasan T, Cincotta AH. Benzophenothiazine and benzoporphyrin derivative combination phototherapy effectively eradicates large murine sarcomas. *Photochem Photobiol.* 1996; 63:229–237. [PubMed: 8657737]
7. Yousef IS, Perozzo R, Schmid I, Ziemiecki A, Schaffner T, Scapozza L, Brunner T, Simon HU. Calpain-mediated cleavage of Atg5 switches autophagy to apoptosis. *Nat Cell Biol.* 2006; 8:1124–1132. [PubMed: 16998475]
8. Medina DL, Di Paola S, Peluso I, Armani A, De Stefani D, Venditti R, Montefusco S, Scotto-Rosato A, Prezioso C, Forrester A, Settembre C, Wang W, Gao Q, Xu H, Sandri M, Rizzuto R, De Matteis MA, Ballabio A. Lysosomal calcium signalling regulates autophagy through calcineurin and TFEB. *Nat Cell Biol.* 2015; 17:288–299. [PubMed: 25720963]
9. Andrzejak M, Price M, Kessel D. Apoptotic and autophagic responses to photodynamic therapy in 1c1c7 murine hepatoma cells. *Autophagy.* 2011; 7:979–984. [PubMed: 21555918]
10. Kessel D. Reversible effects of photodamage directed toward mitochondria. *Photochem Photobiol.* 2014; 90:211–213.
11. Kessel D, Luo Y. Photodynamic therapy: a mitochondrial inducer of apoptosis. *Cell Death Differ.* 1999; 6:28–35. [PubMed: 10200545]

12. Xia HG, Zhang L, Chen G, Zhang T, Liu J, Jin M, Ma X, Ma D, Yuan J. Control of basal autophagy by calpain1 mediated cleavage of ATG5. *Autophagy*. 2010; 6:61–66. [PubMed: 19901552]
13. Luo S, Rubinsztein DC. Atg5 and Bcl-2 provide novel insights into the interplay between apoptosis and autophagy. *Cell Death Differ*. 2007; 14:247–1250.
14. Price M, Heilbrun L, Kessel D. Effects of the oxygenation level on formation of different reactive oxygen species during photodynamic therapy. *Photochem Photobiol*. 2013; 89:683–686. [PubMed: 23216021]
15. Rubinsztein DC, Cuervo AM, Ravikumar B, Sarkar S, Korolchuk V, Kaushik S, Klionsky DJ. In search of an “autophagometer”. *Autophagy*. 2009; 5:585–589. [PubMed: 19411822]
16. Kessel DH, Price M, Reiners JJ Jr . ATG7 deficiency suppresses apoptosis and cell death induced by lysosomal photodamage. *Autophagy*. 2012; 8:1333–1341. [PubMed: 22889762]
17. Reiners JJ Jr, Agostinis P, Berg K, Oleinick NL, Kessel D. Assessing autophagy in the context of photodynamic therapy. *Autophagy*. 2010 Jan; 6(1):7–18. [PubMed: 19855190]
18. Kim I, Lemasters JJ. Mitophagy selectively degrades individual damaged mitochondria after photoirradiation. *Antioxid Redox Signal*. 2011; 14:1919–1928. [PubMed: 21126216]
19. Rodriguez ME, Zhang P, Azizuddin K, Delos Santos GB, Chiu SM, Xue LY, Berlin JC, Peng X, Wu H, Lam M, Nieminen AL, Kenney ME, Oleinick NL. Structural factors and mechanisms underlying the improved photodynamic cell killing with silicon phthalocyanine photosensitizers directed to lysosomes versus mitochondria. *Photochem Photobiol*. 2009; 85:1189–1200. [PubMed: 19508642]
20. Vinod V, Padmakrishnan CJ, Vijayan B, Gopala S. ‘How can I halt thee?’ The puzzles involved in autophagic inhibition. *Pharmacol Res*. 2014; 82:1–8. [PubMed: 24657238]
21. Miki Y, Akimoto J, Moritake K, Hironaka C, Fujiwara Y. Photodynamic therapy using talaporfin sodium induces concentration-dependent programmed necroptosis in human glioblastoma T98G cells. *Lasers Med Sci*. 2015; 30:1739–1745. [PubMed: 26109138]
22. Harris IS, Brugge JS. Cancer: The enemy of my enemy is my friend. *Nature*. 527:170–171. [PubMed: 26503052]
23. Piskounova E, Agathecleous M, Murphy MM, et al. Oxidative stress inhibits distant metastasis by human melanoma cells. *Nature*. 527:186–191. [PubMed: 26466563]

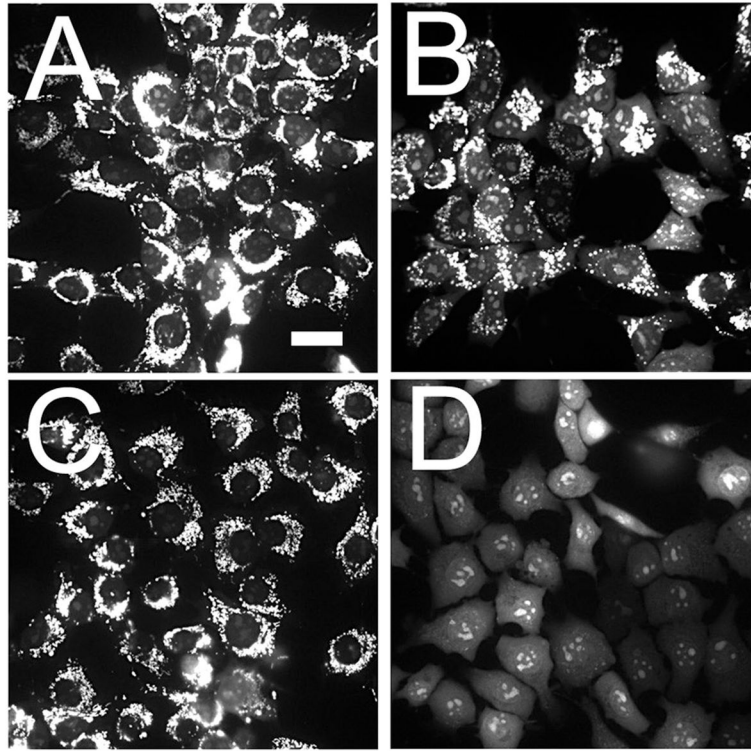


Figure 1. Effect of a lower NPe6 concentration together with a higher light dose on the ability of lysosomal photodamage to potentiate the loss of Ψ_m . Cells were labeled with mitotracker orange (MTO) as described in the text. A, control (untreated) cells; B, after a photodynamic therapy (PDT) dose involving benzoporphyrin derivative (BPD) alone (37.5 mJ/cm^2); C, NPe6 ($20 \mu\text{M}$, 180 mJ/cm^2); D, sequential PDT: both agents present with 660 nm light preceding 690 nm light. (White bar in panel A = $20 \mu\text{m}$).

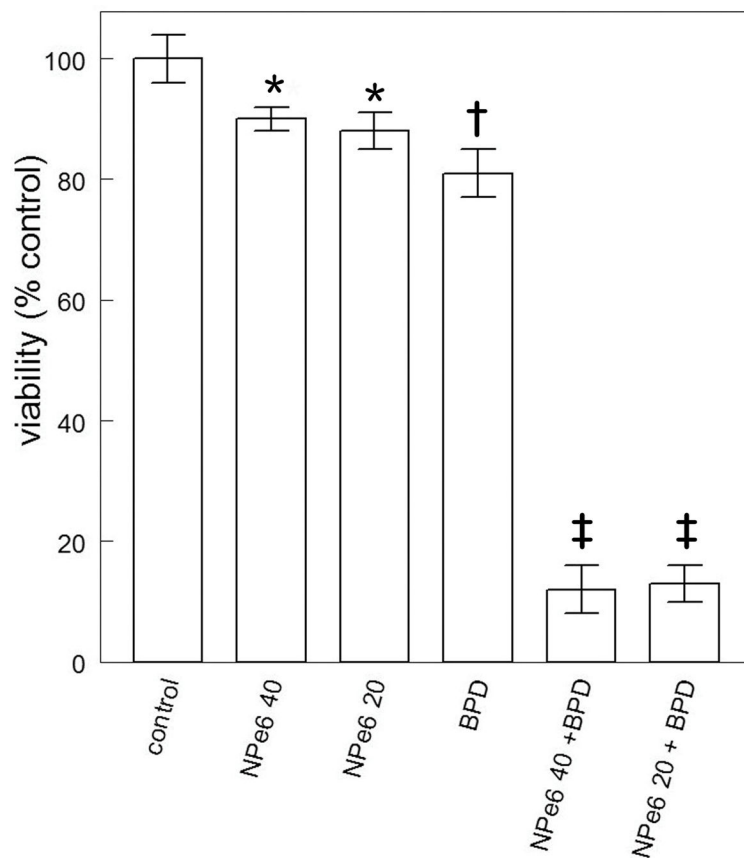


Figure 2. Clonogenic studies showing the efficacy of sequential photodynamic therapy (PDT) treatments using the two different NPe6 protocols (see legend to Fig. 1) followed by benzoporphyrin derivative (BPD)-induced photodamage. *Statistically different from controls ($p < 0.1$); † statistically different from controls ($p < 0.05$); ‡ statistically different from all other groups ($p < 0.001$) by unpaired Student's t-test.

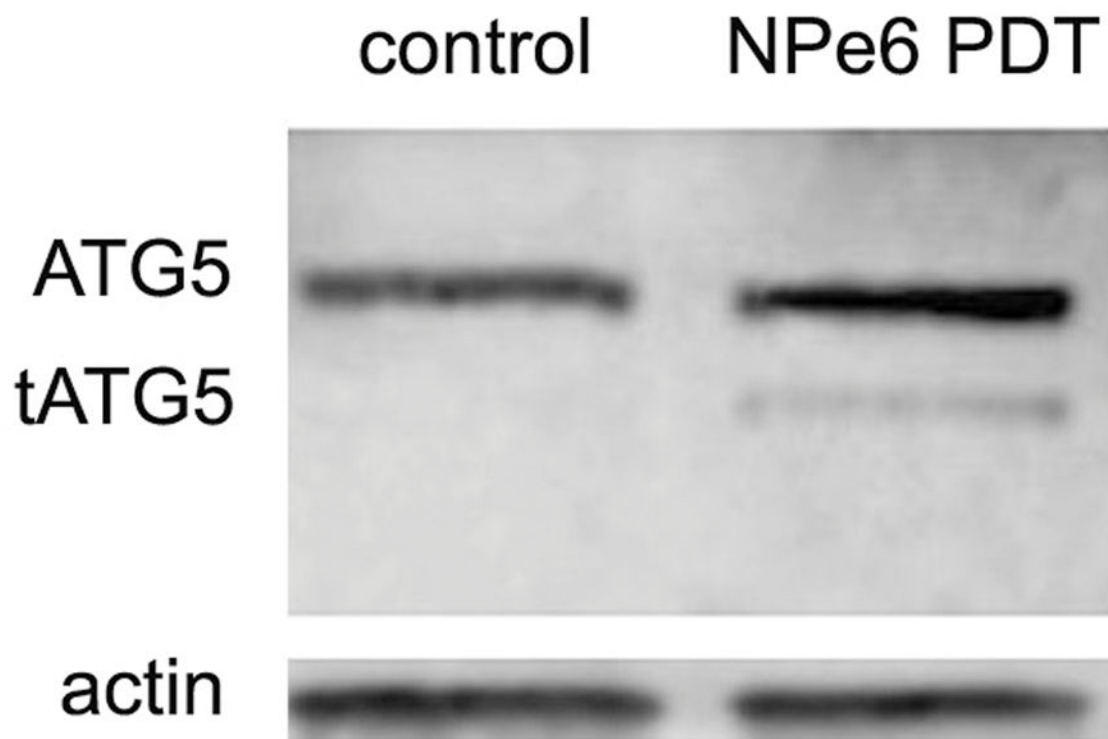


Figure 3.

Effect of low-dose NPe6 photodamage on cleavage of ATG5 to a 24 kDa fragment. After incubation for 60 min with 40 μ M NPe6, cells were exposed to 90 mJ/cm^2 light at 660 ± 10 nm, then collected for analysis.

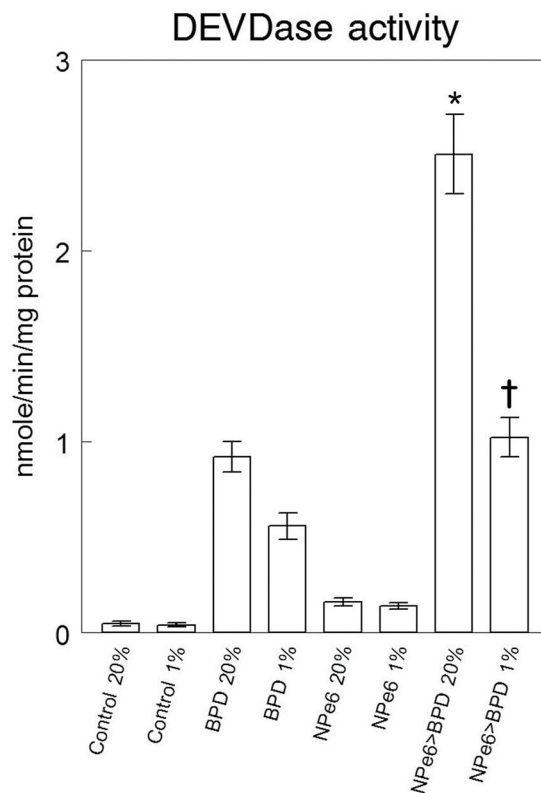


Figure 4.

Activation of caspases 3/7 as a function of the oxygenation level during irradiation indicating partial reversal of effects of hypoxia by prior lysosomal photodamage. Cells were loaded with NPe6 (20 μ M, lanes 5–8) and benzoporphyrin derivative (BPD) (0.5 μ M, lanes 3, 4, 7, 8) and irradiated as specified in the legend to Fig. 1. Lanes 1 and 2 were untreated controls. Irradiation then occurred in an atmosphere of 20% (lanes 1, 3, 5, 7) or 1% (lanes 2, 4, 6, 8) oxygen. DEVDase activity was assessed by a fluorescence assay 2 h later. Data represent average \pm SD for 3 determinations. *Statistically different from BPD PDT in 20% oxygen ($p < 0.001$); † statistically different from BPD PDT in 1% oxygen ($p < 0.01$) by unpaired Student's t-test.

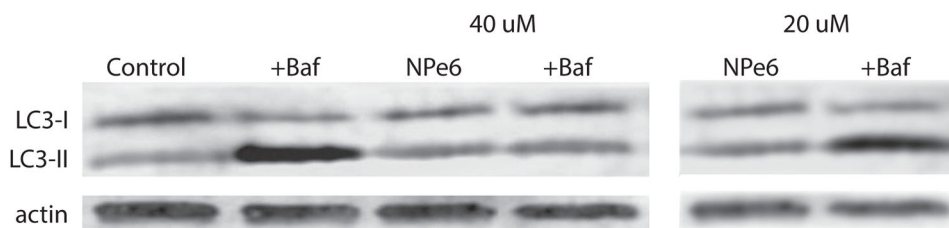


Figure 5. Western blot showing the autophagic flux monitored by conversion of LC3-I to LC3-II over a 1 h interval. NPe6 concentrations were 20 or 40 μ M. Incubations were carried out in the absence of light.